International Journal of Thermal Technologies
E-ISSN 2277 – 4114
Available at http://inpressco.com/category/ijtt/

Research Article

Nano Technology Enhanced Performance of a- $(GeS_2)_{100-x}Ga_x$ /Ge,n,p-Si Hereterojunction

Bushra A.Hasan†, R.M.S.Al-Haddad†, Eman M. Nasir†* and M.A.Kadhem‡

†University of Baghdad, College of Science, Department of Physics, Iraq
‡University of Karbula, College of Science, Department of Physics, Iraq

Accepted 20 March 2015, Available online 31 March 2015, **Vol.5, No.1 (March 2015)**

Abstract

The $(GeS_2)_{100-x}Ga_x$ thin films have been prepared by thermal evaporation under vacuum of (10^{-5} Toor) with thickness (≈ 50nm) at different substrate like glass, single crystal Ge, Si n and p – type at room temperature. We devoted in this work on the effect of gallium concentration (0,6,12 , and 18%)on the optical properties of $(GeS_2)_{100-x}Ga_x$ thin films like (the optical energy gap (E_g),the optical constants (the refractive index (n) ,the extinction coefficient (k) and the real (ε_1) and the imaginary (ε_2) part of dielectric constant. The optical energy gap values were found to decrease in regular manner with increase of Ga concentration of ternary compound in opposite with the optical constants which showed a systematic decrease with increase Ga concentration. The Energy Dispersive x-ray fluorescence (EDX) analysis revealed that thin films has a nearly stoichiometric composition. In this work, the effect of gallium concentration on performance of$(GeS_2)_{100-x}Ga_x$ /n-Si, $(GeS_2)_{100-x}Ga_x$ /p-Si and $(GeS_2)_{100-x}Ga_x$ /p-Ge heretojunctions had been investigated using nano layer. The optimized device has an efficiency of ~20% at room temperature. Investigations on the optimized device showed that gallium concentration has significant effect on the photovoltaic performance. The outcomes result indicates that the photocurrent of and short circuit voltage V_{oc} of the prepared heterojunctions increase in the first and then decreases with increasing of gallium concentration.

Keywords: *$(GeS_2)_{100-x}Ga_x$ alloys, thin films, vacuum evaporation, Heterojnction*

Introduction

Amorphous chalcogenides are very well known semiconductor materials. Due to their high transmittance in the IR spectral region and other interesting optical properties, they are used in the fabrication of a great number of optical devices (D. Minkov *et al*,1987). In general these materials are often preferred over crystalline compounds with similar properties because of their favorable mechanical and interfacing properties. Furthermore , the lack of long-range –order (LRO) make it possible to modify their optical properties to a specific technological application by changing their chemical composition .Consequently, the investigation of the compositional dependence of their optical properties is important to get a better understanding of the mechanisms underlying these phenomena and also to improve their interesting technological applications. To the best of our knowledge, the behavior of thermally evaporated $(GeS_2)_{100-x}Ga_x$ /n,p-Si,Ge, solar cells under diffused white light in terms of its junction characteristics have not been reported yet. In the previous study, we report the fabrication of a stoichiometric $(GeS_2)_{100-x}Ga_x$ thin film by thermal evaporation and its structural, optical and electrical characterizations. Their dark *I–V* characteristic was analyzed to understanding the role of junction ideality on the device performance. We report the compositional dependence of the basic optical properties and band gap, correlation between the composition and the optical properties, photovoltaic effect .In the present study we try to investigate the effect of lowering thickness of p-type layer on the optical and photovoltaic effect of the $(GeS_2)_{100-x}Ga_x$ /n,p-Si,Ge heterojunctions.

Experimental details

The bulk samples of $(GeS_2)_{100-x}Ga_x$ were prepared by quenching technique. The exact amount of high purity (99.999%)(Ge, S and Ga) elements accordance with their atomic percentages (GeS_2, $(GeS_2)_{94}Ga_6$, $(GeS_2)_{88}Ga_{12}$ and $(GeS_2)_{82}Ga_{18}$ are weighed using an electronic balance with the least count of (10^{-4} g). The material was then sealed in evacuated (~10^{-5} Torr) quartz ampoule (length ~ 25 cm and internal diameter ~ 8 mm). The ampoules containing material are heated to 1100 °C for GeS_2 and 850°C for $(GeS_2)_{94}Ga_6$, $(GeS_2)_{88}Ga_{12}$ and $(GeS_2)_{82}Ga_{18}$ for 5 hours .The temperature of the furnace was raised at a rate of 10

*Corresponding author: **Eman M. Nasir**

°C/min. During heating the ampoules are constantly rocked. This is done to obtain homogeneous glassy alloys. After that the obtained melt was rapidly quenched into water . Amorphous $(GeS_2)_{100-x}Ga_x$ thin films with different gallium concentration were prepared using thermal evaporation. The evaporation carried out using Edward coating unit (model E306A). During the evaporation of the films, the pressure in the system was $4x10^{-5}$ Torr. All the samples were prepared under constant condition [pressure, rate of deposition (2.33nm/sec), substrate temperature (room temperature) and thickness). In this work, corning glass substrates, single crystals of (111) orientation n-Si, (001) orientation p-Si and (111) orientation p-Ge are employed. The substrates were subjected to several cleaning stages. Single crystal Silicon and Germanium wafers were cleaned using etching process which is summarized as follows :(i). Ge wafers were immersed and stirred in a chemical solution consists of 1 ml HF, 3 ml H NO_3 ,5 ml CH_3COOH, while Si wafers immersed and stirred in a chemical solution consists of 1 ml HF, 3 ml H NO_3 for (1–2) minutes.(ii). These specimens were then rinsed by distilled water several times.(iii).Finally, the specimens were dried using soft paper.The most approximate method that is used to determine the amount of the materials which are required to certain evaporation is the weighting method. The quantity of material that is needed to achieve films thickness t is given by:

$$m = 2\pi\rho_o R'^2 t$$

Where:
m is the mass of material, R′ is the distance between the source and the sample holder, ρ_o is the density of the material is the thin film thickness. The method has high error ratio, the actual thicknesses were obtained by optical interference fringes. Fizeau fringes of equal thickness are obtained; the film thickness (t) is given by:

$$t = \frac{\lambda}{2} \cdot \frac{\Delta X}{X} \quad (1)$$

Where ΔX is the shift between the interference fringes, X is the distance between the interference fringes and λ is the He:Ne wavelength (6320 Å). Compositional analysis of $(GeS_2)_{100-x}Ga_x$ alloys was carried out by EDAX analysis. Gallium concentration in the alloys was varied from 0 to 18 wt.%. The atomic percentage ratio of Ge, S, and Ga in alloys is listed in Table 1, it shows that the samples are in good stoichiometric ratio. The concentration of the elements (Ge, S and Ga) in the alloys was examined by energy dispersive x-ray fluorescence (EDX) technique depending on the standard of these elements.

Structural analysis of the $(GeS_2)_{100-x}Ga_x$ thin films was made using X-ray diffractometer with CuK_α radiation (λ=1.5418 Å) in the scanning angle (2θ) from 20° to 60°. The surface morphology and roughness were examined by atomic force microscopy (AFM) under ambient condition. The optical transmission spectra of the as-deposited and annealed films were recorded using a Perkin-Elmer Lambda 35 UV-VIS double-beam spectrophotometer in the wavelength range 300-1100 nm. The observed transmittance data were corrected relative to optically identical uncoated glass substrate. The transmission spectrum curve was used for calculating the optical constants of the investigated samples. The optical constants are very important parameters because they describe the optical behavior of the materials. The absorption coefficient of the material is a very strong function of the photon energy and band gap energy. Absorption coefficient represents the attenuation that occurs in incident photon energy on the material for unit thickness, and the main reason for this attenuation is attributed to the absorption processes (S. Elliott *et al*, 1984; R. *Elliot et al*, 1974). Optical constants included refractive index (n), extinction coefficient (k), and real (ε_r) ,and imaginary parts (ε_i) of dielectric constant.

Table 1 Quantitative analysis of Ge, S and Ga by using EDAX for $(GeS_2)_{100-x}Ga_x$

Alloy	Calculated			observed		
	Ge	S	Ga	Ge	S	Ga
(GeS_2)	33.333	66.667	0.000	33.196	66.392	0.000
$(GeS_2)_{94}Ga_6$	31.333	62.667	6.000	31.183	62.367	5.970
$(GeS_2)_{88}Ga_{12}$	29.333	58.667	12.000	29.262	58.524	11.940
$(GeS_2)_{82}Ga_{18}$	27.333	54.667	18.000	27.198	54.397	17.910

The complex refractive index (n_c) is defined as (J. Millman , 1979):

$$n_c = n - ik \quad (2)$$

and it is related to the velocity of propagation (v), and light velocity (c) by:

$$v = c/n_c \quad (3)$$

The refractive index value can be calculated from the formula (B.Ray, 1969):

$$n = \left(\frac{4R}{(R-1)^2} - k^2\right)^{\frac{1}{2}} - \frac{(R+1)}{(R-1)} \quad (4)$$

Where R is the reflectance, and can be expressed by the relation (J. Millman , 1979):

$$R = \frac{(n-1)^2 + k^2}{(n+1)^2 + k^2} \quad (5)$$

The extinction coefficient, which is related to the exponential decay of the wave as it passes through the medium, is defined as (S.Sze, 1981):

$$k = \frac{\alpha\lambda}{4\pi} \quad (6)$$

Where λ is the wavelength of the incident radiation and (α) is given by (S.Sze, 1981):

$$\alpha = 2.303\frac{A}{t} \qquad (7)$$

Where A is the absorbance and t is the sample thickness. The real and imaginary part of dielectric constant can be calculated by using the following equations (S.Sze, 1981):

$$(n-ik)^2 = \varepsilon_r - i\varepsilon_i \qquad (8)$$

Where

$$\varepsilon_r = n^2 - k^2 \qquad (9)$$

and $\varepsilon_i = 2nk$ (10)

The solar cell structures fabricated in this study consists of (from the bottom) an Al layer as the back contact (≈ 200 nm), single crystal wafers (n-, p-type Si and p-type Ge) and $(GeS_2)_{100-x}Ga_x$ layer thickness of 50 nm, all these layers are prepared by thermal evaporation. The wires were connected by silver baste. The electrical measurements for $(GeS_2)_{100-x}Ga_x$ /n-Si, $(GeS_2)_{100-x}Ga_x$ /p-Si and $(GeS_2)_{100-x}Ga_x$ /p-Ge Heterojunction, includes current-voltage characteristic measurements in the dark and under illumination conditions as well as capacitance voltage characteristic measurements were done. The capacitance of the Heterojunction is measured as a function of the reverse bias voltage at the range (0-1.5) Volt with fixed frequency of 1 kHz using HP-R2C unit model 4274A and 4275A multi-frequency LRC meter. Capacitance voltage measurements can be manipulated to yield a number of parameters such as: type of the junction (abrupt or graded), built - in voltage (V_{bi}), carrier concentration and the width of the junction (depletion layer).The charge-carrier density (N_d) and width of the depletion layer (w) for both devices are calculated by the following equations :

$$N_d = \frac{2}{q\varepsilon_s}[1/d(A^2/C^2))/dV] \qquad (11)$$

When A the active area (0.9cm^2).The current-voltage measurements in the dark were done for the$(GeS_2)_{100-x}Ga_x$ /n-Si, $(GeS_2)_{100-x}Ga_x$ /p-Si and $(GeS_2)_{100-x}Ga_x$ /p-Ge heterojunction using Keithley digital electrometer 616 and D.C. power supply .The bias voltage was varied in the range of (0 – 1.5) Volt in the case of forward and reverse bias .From plots of the relation between the forward current and bias voltage, the ideality factor β can be determined by the relation defined as:

$$I_F = I_S \exp\frac{qV}{\beta k_B T} \qquad (12)$$

Where I_s is the saturation current, and is the ideality factor parameter related to the various physical properties of the heterojunction having a value between 1 and 2. We can calculate the width of the depletion region by:

$$w = \frac{2\varepsilon_s V_{bi}}{qN_d} \qquad (13)$$

Where ε_s is the semiconductor permittivity for the two semiconductor materials and it is given by:

$$\varepsilon_s = \frac{\varepsilon_n \varepsilon_p}{\varepsilon_n + \varepsilon_p} \qquad (14)$$

I-V measurements were made for$(GeS_2)_{100-x}Ga_x$ /n-Si, $(GeS_2)_{100-x}Ga_x$ /p-Si and $(GeS_2)_{100-x}Ga_x$ /p-Ge heterojunction when they were exposed to Halogen lamp light Philips (120W) with intensity 106 mW/cm^2 using Keithley Digital Electrometer 616, voltmeter and D.C. power supply under reverse bias voltage which was in the range (0-1.5) Volt.

Results and Discussion

X-ray diffraction pattern (XRD) was used to study the structure properties of $(GeS_2)_{100-x}Ga_x$ thin films. Fig. 1 shows a typical XRD pattern derived for the as-deposition thin film samples. The figure declares the absence of any sharp diffraction lines, indicating that amorphous nature of $(GeS_2)_{100-x}Ga_x$ in thin film form. Figure 2 shows the three-dimensional (3D) surface morphology of $(GeS_2)_{100-x}Ga_x$ thin films. From this, it is concluded that the films have uniformly or an uniformly distributed spherical or distorted spherical grains giving the smooth surface morphology. The deformed shaped grains have been observed for the GeS_2 and $(GeS_2)_{94}Ga_6$ while nearly spherical grains were observed for the other two film samples. The calculated values of surface roughness and the grain sizes are summarized in Table 2. It has been observed that a minimum surface roughness has been found for the GeS_2 sample while the $(GeS_2)_{88}Ga_{18}$ sample has the maximum value. Similarly, the smallest height of the grains were found for the GeS_2 (2.823 nm) and largest for the $(GeS_2)_{82}Ga_{18}$ (approximately 18.66 nm) film samples. Low thickness of the thin films resulted in the approaching of height of the grains and surface roughness.

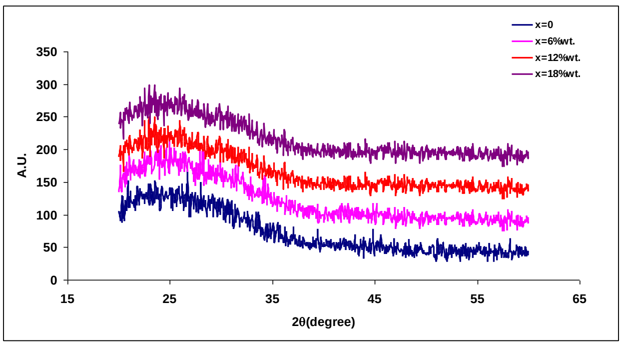

Fig.1 X-ray diffraction pattern for $(GeS_2)_{100-x}Ga_x$ thin films with different Ga concentration

Table 2 Average height of the grains and average roughness for $(GeS_2)_{100-x}Ga_x$ with different Ga concentration

Thin film Sample	Ave. height of the grains (nm)	Ave. Roughness (nm)
GeS_2	2.82	2.58
$(GeS_2)_{94}Ga_6$	5.21	10.1
$(GeS_2)_{88}Ga_{12}$	15.40	12.8
$(GeS_2)_{82}Ga_{18}$	18.66	13.1

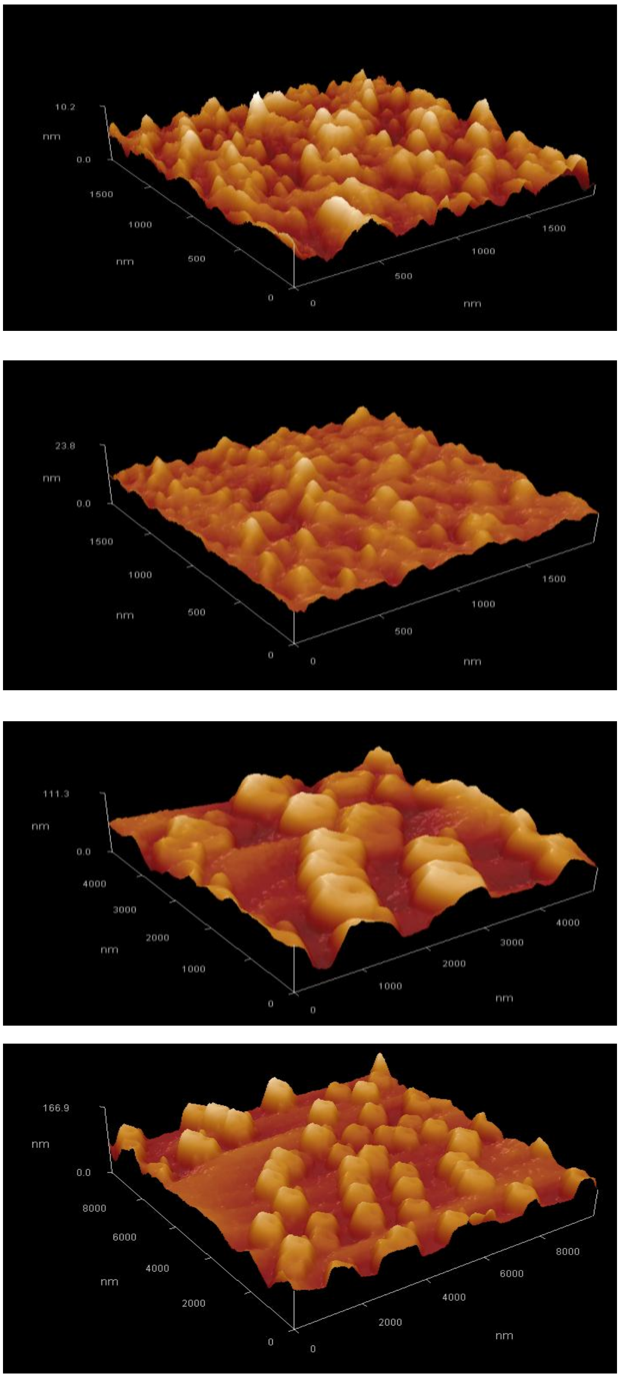

Fig.2 Three-D AFM images of $(GeS_2)_{100-x}Ga_x$ thin films with different Ga concentration

The optical study for $(GeS_2)_{100-x}Ga_x$ with ≈50nm in thickness film deposited on glass substrate with different Gallium contents (x= 0, 6, 12 and 18) was carried out in the wavelength range 300–1100 nm. The transmission spectrum in the wavelength range 300-1100 nm was used to calculate the optical constants of $(GeS_2)_{100-x}Ga_x$ thin films. Fig. 3 shows the transmission spectrum obtained for investigated sample at room temperature. The film exhibited a sharp absorption and the optical transparency in the wavelength range 700-1100 nm was more than 80 %. The oscillations in the transmission spectrum are caused by optical interference arising due to difference of refractive index of film with glass substrate and the interference of multiple reflections originated from film and substrate surfaces. The figure indicate the shifting of absorption edge to longer wavelength or lower energy indicating decreasing of E_g^{opt} with increasing gallium concentrations .On the other hand the transmittance pattern of all deposited thin films of different ternary system increases with increasing (λ), Indeed T decreases form (0.94 to 0.89)when gallium content increases from 0 to 18%.

This result in argument with (K. Palanjyan *et al,* 2013). The shifts of transmittance toward (lower energies) accompanied gallium increment explained according that increasing of gallium concentration creates new states in band gap of the of the amorphous system which reflect as shifting of the absorption edge toward lower energies consequently to the shift of the optical energy gap toward lower values as will be seen in the next section.

The Tauc plot for the as-deposited stoichiometric $(GeS_2)_{100-x}Ga_x$ films is shown in figure 4. It is obtained from the transmittance spectra measured by the UV–Visible is spectrometry in the wavelength range of 300–1100 nm. The direct optical band gaps (Eg) of the thermally evaporated $(GeS_2)_{100-x}Ga_x$ thin films were thus determined to be about 2.9 eV, decreases to 1.65 eV. This result is attributed to increase of the absorption coefficient, in turn to an additional shift of the optical absorption edge in the direction of lower energies. The almost linear decrease of the band gap with gallium content is attributed also to the structural transformation in the films after Ga introducing. The incorporation of Ga clusters in the Ge-S matrix is connected with an increase of the disorder and an increase in the number of localized states within the band gap. According to (N. Mott *etal,* 1982) the presence of high density of localized states in the band structure is responsible for lower values of the optical gap. It seems that our experimental data agree well with Davis and Mott suggestion. The obtained values of (E_g) for as deposited films $(GeS_2)_{100-x}Ga_x$ listed in table.1. It clear that the values of Eg^{opt} are higher those obtained in literature for higher thickness, this attribute to decrease the particle size (confinement effect), this result is agreement with (. R. Todorov *et al*, 2003; K. Petkov *et al*, 2002; Jia Zhu *et al*, 2009). The result explained according to the relation $\Delta E \approx \frac{h^2}{m^* t^2}$ where ΔE is the reduction in the energy gap , t is the thickness.

The wavelength (λ) dependence of the refractive index (n) for as deposited $(GeS_2)_{100-x}Ga_x$ thin films with different Gallium concentration (x= 0, 6, 12 and 18) is shown in Fig.5. It is clear that (n) values decreases with increase of (λ) of the incident photon ,on the other hand it is found from Fig.5 that increase of Ga concentration from (0 to 18% wt.) increases (n) values ,indeed the refractive index values increases from (1.412 to 1.703)when Ga concentration increases from 0 to 18%, (see table 3). This behavior reflects the decrease of transmittance i.e. the sample becomes more opaque to the incident (λ) as expected from the simultaneous decrease of the energy gap. In order to compare our results with a published data the value of (n =1.412) were determined at (λ=600 nm), while (Z. Ivanova *et al*, 2001) obtained n=2.55 at λ=900 nm for $Ge_{31}S_{61}Ga_8$ films, the difference attributed to different composition and wavelength.

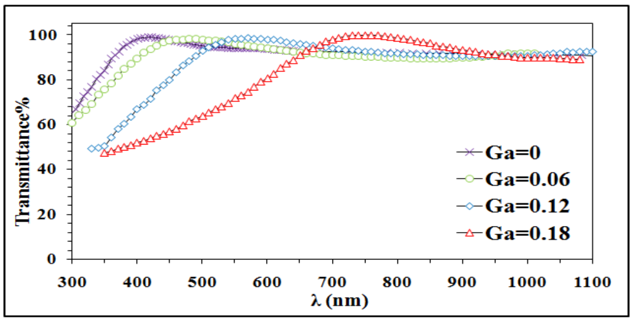

Fig.3 The transmission variation with the wavelength for as deposited $(GeS_2)_{100-x}Ga_x$ films thickness of ≈50nm

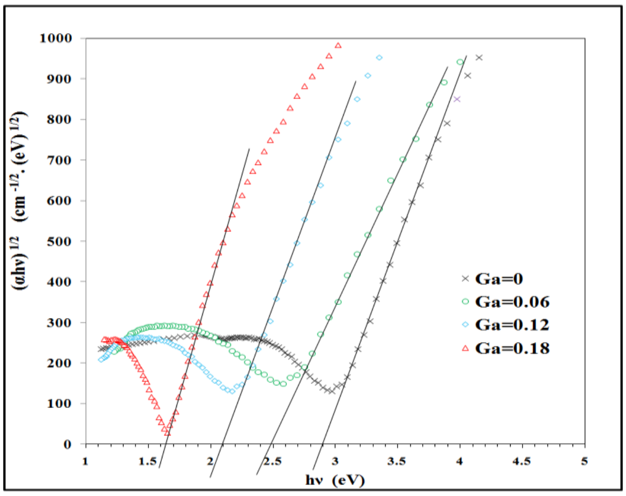

Fig.4 Tauc plot of as-deposited $(GeS_2)_{100-x}Ga_x$ film on the glass thickness of ≈50nm

The dependence of extinction coefficient (k)on the wavelength(λ) is shown in Fig.6.It is remarked that the values of (k) are varied with (λ) ,indeed (k) for as deposited films with different gallium concentration increases, moreover it is found that (k) values increases from (0.146 to 0.515) at (λ=600 nm) (see table (1).This behavior is related with the corresponding absorption coefficient(α)according to equation (6) , hence (α) are revealed increment with increase of (Ga) concentration.

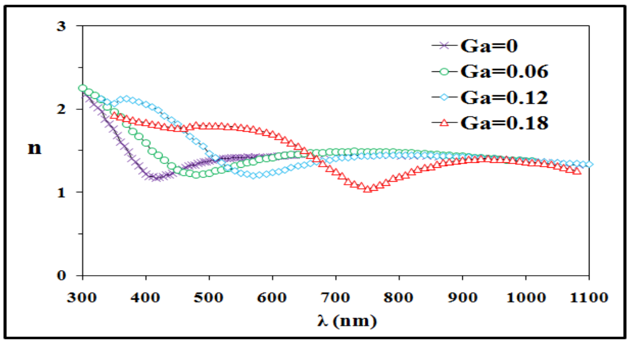

Fig.5 Variation of refractive index with the wave length for as deposited $(GeS_2)_{100-x}Ga_x$ films thickness of ≈50nm

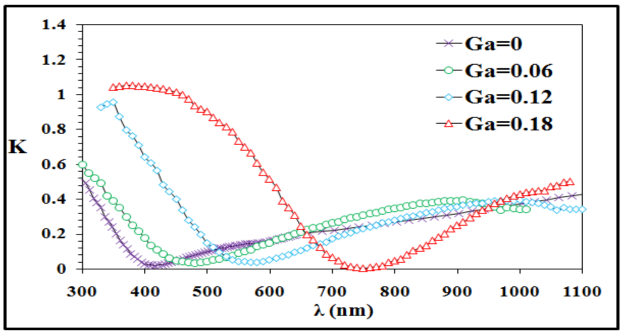

Fig.6 Variation of extinction coefficient (k) with wavelength for as deposited $(GeS_2)_{100-x}Ga_x$ films) thickness of ≈50nm

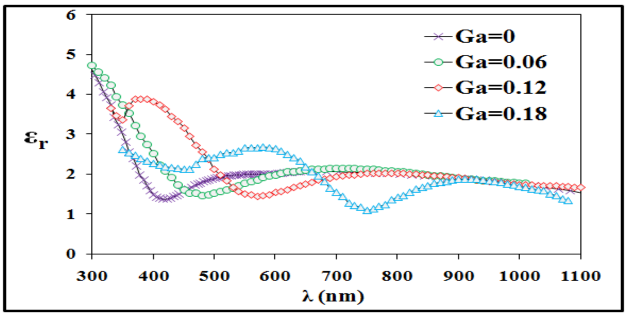

Fig.7 Variation of ε_r with the wavelength for as deposited $(GeS_2)_{100-x}Ga_x$ films thickness of ≈50nm

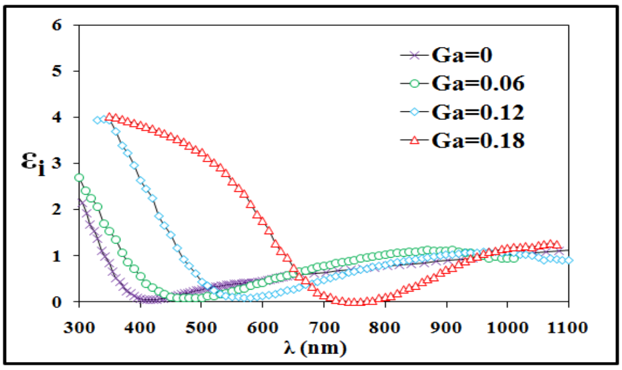

Fig.8 Variation of ε_i with the wavelength for as deposited $(GeS_2)_{100-x}Ga_x$ films thickness of ≈50nm

The real (ε_r) and imaginary part (ε_i) of the dielectric constant for as deposited $(GeS_2)_{100-x}Ga_x$ thin films with different gallium concentration as function of wavelength are shown in Fig.(7 and 8) . It is clear that the variation of (ε_r) mainly depend on the values of (n^2) as a results of small values of (k^2) comparison with (n^2), while (ε_i) mainly depend on the (k) values which are related to the variation of absorption coefficient.

Table 3 Optical energy gap and optical constants at λ=600 nm for as deposited $(GeS_2)_{100-x}Ga_x$ films for different Gallium content (x= 0, 6, 12 and 18) thickness of ≈50nm

x	0	6	12	18
T%	94	94	93	81
E_g^{opt}(eV)	2.9	2.53	2.1	1.65
k	0.146	0.148	0.053	0.515
n	1.412	1.415	1.243	1.703
ε_r	1.97	1.98	1.54	2.63
ε_i	0.41	0.42	0.13	1.75

Characteristics of $(GeS_2)_{100-x}Ga_x$ /n-Si, $(GeS_2)_{100-x}Ga_x$ /p-Si and $(GeS_2)_{100-x}Ga_x$ /p-Ge heterojunctions

The junction capacitance variations of the reverse bias of $(GeS_2)_{100-x}Ga_x$ /n-Si, $(GeS_2)_{100-x}Ga_x$ /p-Si and $(GeS_2)_{100-x}Ga_x$ /p-Ge heterojunction prepared with different gallium concentration (0,6,12, and 18%) are plotted in Figs. 9 a-c. It is clear that the capacitance increase with the increase of reverse bias, this is due to increase in the depletion layer width , which lead to an increase in built in voltage values .On the other hand the capacitance increase with the increase of gallium content . This behavior ascribes to the increase of carrier concentration as a result of reduce the potential barrier which lead to increase the capacitance and reduction of width layer. The linear dependence of C^{-2}-V curves gives us an indication that the impurity profile near the junction is abrupt. Table. 4 illustrate the parameters measured in this work. It is obvious that built in voltage decreases with the increase of gallium concentration; this can be attributed to reduction of Eg as result of gallium concentration increment which leads to reduces V_{bi}., since V_{bi}. Is related with V_{oc} and the maximum value of the latter is close to the energy gap. The carrier concentration increases with increase of gallium concentration. Fig.10 show the semi-log relation of forward dark current and the biasing voltage (0-0.2)Volt for $(GeS_2)_{100-x}Ga_x$ /n-Si, $(GeS_2)_{100-x}Ga_x$ /p-Si and $(GeS_2)_{100-x}Ga_x$ /p-Ge respectively prepared with different gallium concentration , It clear that the there are two region the first the recombination current is dominated while the tunneling current is dominated at the second region. hence it is obey the recombination- tunneling mechanism. The significant feature of this figure is the non ohmic behavior, where current flow in the forward biasing, but very law current flows in reverse biasing. It is obvious from this figure that the value of the current decreases with increasing of gallium concentration, however the dark current show significant increase at x=12%. In general the forward dark current is generated due to the flow of majority carriers and the applied voltage injects majority carriers which lead to the decrease of the built - in potential, hence decreases the width of depletion layer.

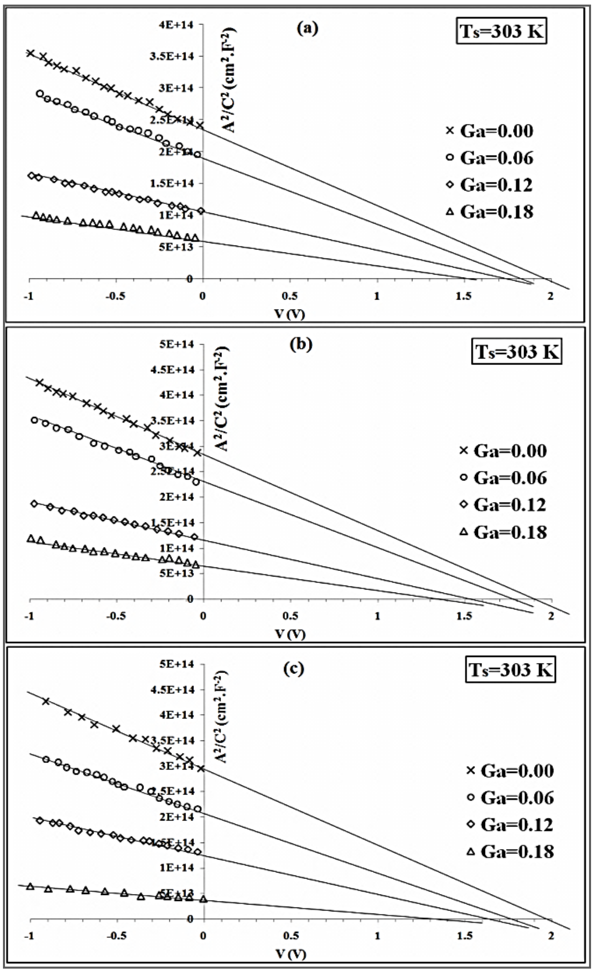

Fig.9 The variation of A^2/C^2 versus the reverse bias voltage for (a) $(GeS_2)_{100-x}Ga_x$/n-Si, (b) $(GeS_2)_{100-x}Ga_x$ /p-Si and (c) $(GeS_2)_{100-x}Ga_x$ /p-Ge heterojunctions with different Ga content

For a p–n junction solar cell, the diode ideality factor (β) is an important parameter that determines the quality of the junction, where β approaching unity is considered ideal. According to the Sah–Noyce–Shockley theory (C. T. Sah *et al*, 1957), an ideality factor $0 < \beta \leq 1$ at low voltages and $\beta \rightarrow 2$ at higher voltages were predicted. The range of β, $1 < \beta < 2$, suggests the presence of surface and interface states at the junction making it non-ideal where the Shockley–Reed–Hall type recombination is probable. The ideality factor $\beta > 2$ has not been covered in this theory; instead, a coupled defect level recombination mechanism has been theoretically predicted [O. Breitenstein *et al*, 2006; A. Schenk *et al*, 1995) and verified experimentally (M.Brotzmann *et al,* 2009). However, the ideality factor $\beta > 6$ is not covered by either of these two theories. It was suggested by

Table 4 Values of V_{bi}, W and N_d for $(GeS_2)_{100-x}Ga_x$ /n-Si, $(GeS_2)_{100-x}Ga_x$ /p-Si and $(GeS_2)_{100-x}Ga_x$ /p-Ge heterojunctions with different Ga content

substrate	x	w*10^{-2} (cm)	N_d*10^{17}cm^{-3}	V_{bi} (V)	β
n-Si	0	9.08	1.79	2	2.8
	6	8.08	2.08	1.85	2.8
	12	6.14	3.67	1.8	2.21
	18	4.54	5.86	1.55	1.99
p-Si	0	9.80	1.41	1.9	2.9
	6	9.26	1.66	1.8	2.9
	12	6.42	3.06	1.55	1.93
	18	4.72	4.40	1.4	1.29
p-Ge	0	10.15	1.53	2	1.07
	6	8.49	1.88	1.8	1.08
	12	7.18	3.19	1.6	1.87
	18	3.17	8.82	1.4	2.65

(M.Brotzmann *et al,* 2009) that an amorphous or disordered interface layer at the junction could lead to such a large value of β where the conduction properties were well explained by the Frenkel–Poole (FP) model (S.Sze, 1981, Z. Xu *et al*, 2012).

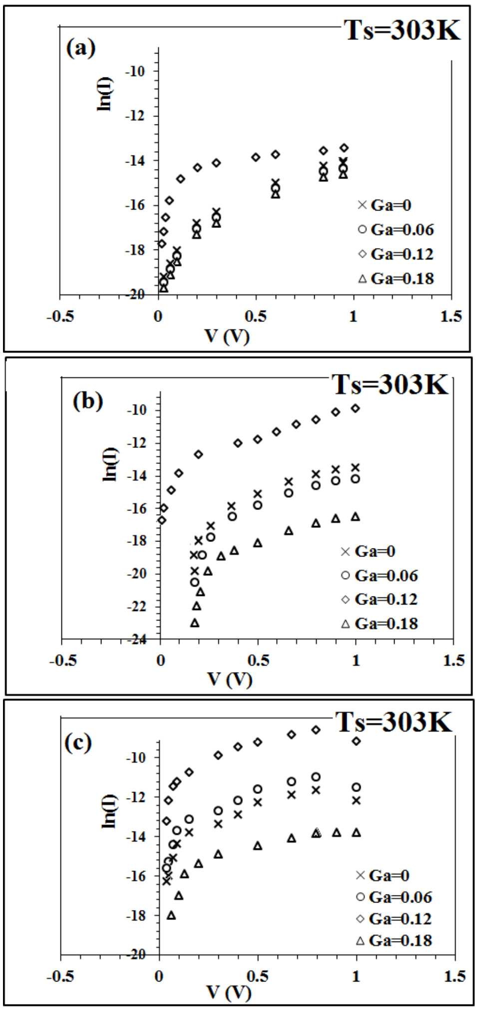

Fig.10 I-V characteristics in dark of (a) nano-$(GeS_2)_{100-x}Ga_x$/n-Si, (b) nano-$(GeS_2)_{100-x}Ga_x$ /p-Si and (c) nano—$(GeS_2)_{100-x}Ga_x$ /p-Ge heterojunctions

Usually, a solar cell fabricated by vacuum process reduced the probability of incorporating defects in the form of interface states, and in turn prevents the recombination of charge carriers. The diode ideality factor β varies in the forward bias region, where β is found to decreases in the range of 2.8–1.99, 2.9-1.29 for $(GeS_2)_{100-x}Ga_x$ /n-Si, $(GeS_2)_{100-x}Ga_x$ /p-Si cells but increases in the range1.07-2.65 for $(GeS_2)_{100-x}Ga_x$ /p-Ge cells with the increase of gallium concentration. As the obtained ideality factor β is little greater than its normal range, $1 < \beta < 2$, it can be inferred that defects exist in the quasi-neutral region as well as in the junction, and are responsible for the recombination of the carriers at the junction.

Interestingly as is well known that, three basic parameters of the solar cells, open-circuit voltage (V_{oc}), short-circuit current (J_{sc}) and F.F, need to be enhanced in order to improve the cell efficiency under the standard illumination condition. In the present case, the cell has been fabricated entirely by thermal evaporation technique which is a high-vacuum process. There is probability of creation band-gap discontinuities over the absorber layer, which in turn has caused a lower V_{oc}. Another source of low V_{oc} could be the surface barrier that was estimated to be about half of the absorber band gap. Secondly, thickness uniformity in the absorber layer could produce a large number of shunting paths for photocurrent, causing deterioration in the FF. The defect density increases with introduction of gallium to the GeS_2 binary system. It caused the diode ideality factor to be more than 2. Another significant source is the series resistance due to a back contact. In this study, we have used the silver paste as a back metal contact, which has may introduce a large series resistance.

The current–voltage characteristics under the white light illumination are shown in figure 11a-c. The extracted device performance parameters are listed in table 5. The measurements were carried out under incident power density equal to (106) mW/cm^2. The current-voltage characteristic under illumination is one of the optoelectronic characteristic for

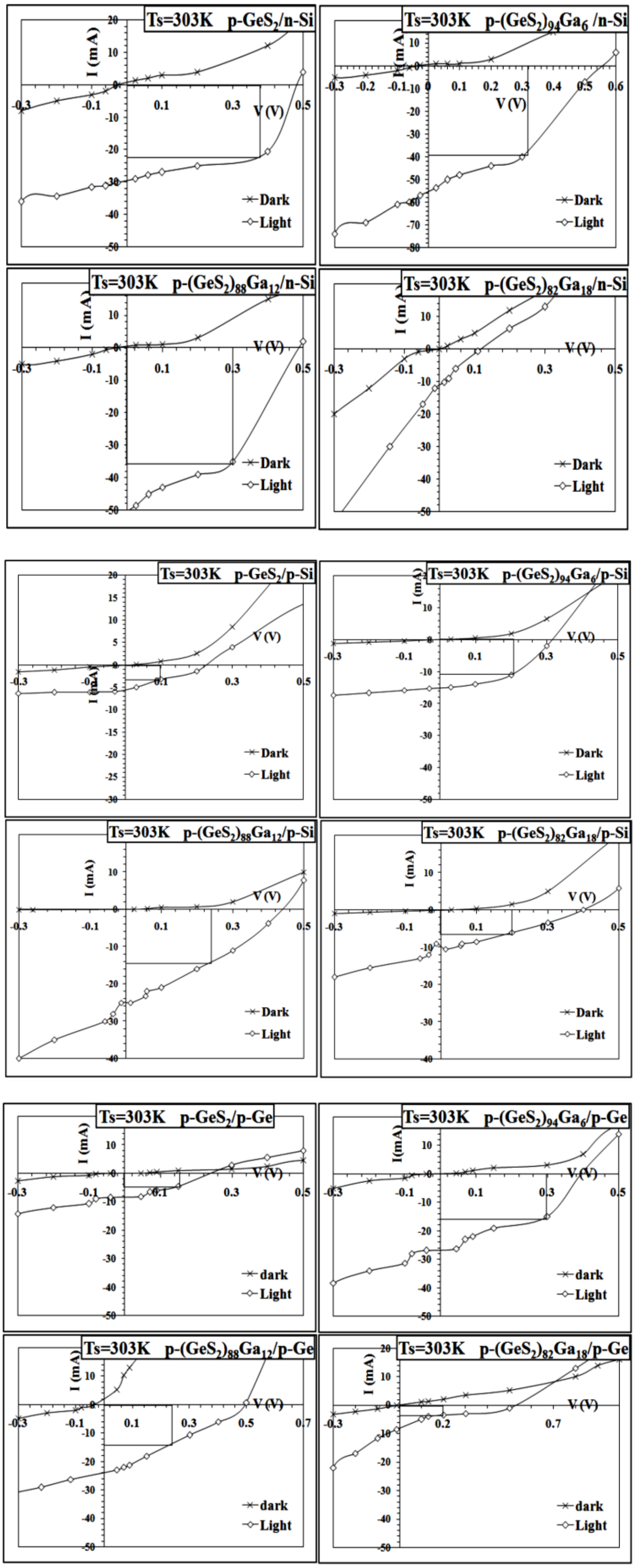

Fig.11 I-V characteristics in dark and light by 105mW/cm^{2}of (a)nano-$(GeS_2)_{100-x}Ga_x$ /n-Si, with different Ga content (b)nano-$(GeS_2)_{100-x}Ga_x$ /p-Si, with different Ga content (c)nano-$(GeS_2)_{100-x}Ga_x$ /p-Si, with different Ga

Table 5 I-V parameters of nano-$(GeS_2)_{100-x}Ga_x$ /n,p-Si, Ge , samples illuminated by 106 mW/cm^2 white light deposited at R.T with different Ga content

Junction	V_{oc} (mV)	I_{sc} (mA)	V_{max} (mV)	I_{max} (mA)	F.F	η%
p-GeS_2/n-Si	480	30	380	24	0.63	11.6
p-$(GeS_2)_{94}Ga_6$/n-Si	480	65	320	49	0.50	19.9
p-$(GeS_2)_{88}Ga_{12}$/n-Si	550	55	320	40	0.42	16.3
p-$(GeS_2)_{82}Ga_{18}$/n-Si	120	12	80	8	-	-
p-GeS_2/p-Si	200	5	100	4	-	-
p-$(GeS_2)_{94}Ga_6$/p-Si	320	15	210	12	0.53	3.2
p-$(GeS_2)_{88}Ga_{12}$/p-Si	440	25	260	15	0.35	5.0
p-$(GeS_2)_{82}Ga_{18}$/p-Si	400	10	200	8	0.40	2.0
p-GeS_2/p-Ge	260	8	180	7	0.61	1.6
p-$(GeS_2)_{94}Ga_6$/p-Ge	400	27	300	18	0.50	6.9
p-$(GeS_2)_{88}Ga_{12}$/p-Ge	500	25	260	15	0.31	5.0
p-$(GeS_2)_{82}Ga_{18}$/p-Ge	500	9	200	5	0.22	1.3

hetrojunction. The photocurrent is considered as an important parameter that plays an effective role in solar cell devices. From these figures it can be observed that the photocurrent increases with increasing the bias voltage due to the reduction of the width of depletion region also it can be seen that the photocurrent in the reverse bias is larger than that in the forward bias. This can be attributed to the fact that the width of the depletion region increases with the increase of the applied reverse bias voltage which leads to the separation of the electron–hole pairs , therefore the photocurrent is a function of the generation and diffusion of carriers. It is obvious that V_{oc} and I_{sc} of $(GeS_2)_{100-x}Ga_x$ /n-Si, $(GeS_2)_{100-xx}Ga_x$ /p-Si declared similar behavior with increase of gallium concentration, i.e. increases but then decreases with increase of gallium concentration, while V_{oc} and I_{sc} of p-$(GeS_2)_{100-x}$ Ga_x/p-Ge increases with the increase of gallium concentration. The ideal efficiency increases primarily due to the increasing of V_{oc} while the photocurrent is increased linearly with the intensity. Is it clear that quantum efficiency of anisotype cells p-$(GeS_2)_{100-x}$ Ga_x/n-Si exceeded that of isotype cells p-$(GeS_2)_{100-x}$ Ga_x/p-Si and p-$(GeS_2)_{100-x}$ Ga_x/p-Ge. Semiconductors used for the heterojuntion solar cell illuminated with light with photon energies well above the band gap energies have a large absorption coefficient. This gives rise to substantial surface recombination and a reduction of the quantum efficiency. One way of decreasing this unwanted absorption is to decrease the thickness of one junction layers. However, this should be achieved without substantially increasing the series resistance of the device because such an increase has the undesired effect. Thus the use of low thickness of the $(GeS_2)_{100-x}$ Ga_x enhanced the solar cell parameters.

Conclusions

The investigation of optical properties of $(GeS_2)_{100-x}Gax$ thin films shows that optical band gap decreases with the gallium introduction into the GeS_2 glassy matrix. The film transparency decreases as gallium is introduced due to the stronger metallic character of the chemical bonds. The reduction of the p-type layer enhanced the efficiency of the prepared cells. Best results of V_{oc} and I_{sc} in these cells are obtained with p-GeS_2/n-Si ,p-$(GeS_2)_{94}Ga_6$/n-Si , and p-$(GeS_2)_{88}Ga_{12}$/n-Si deposited at R.T .In this paper we showed that in $(GeS_2)_{100-x}Ga_x$ /n-Si, $(GeS_2)_{100-x}Ga_x$ /p-Si and $(GeS_2)_{100-x}Ga_x$ /p-Ge heterojunctions the use of n-Si base results in a higher V_{oc}. In general value of I_{sc} is relatively higher if $(GeS_2)_{100-x}Ga_x$ thin films with medium gallium content i.e. 6,12% rather than with high or low content. The prepared cells produce a higher Isc, due to the reduction in the optical band gap and the resulting efficient optical absorption. Thermally deposition method permitted the fabrication of cells of area 0.9 cm^2.

References

D. A. Minkov, E. Vateva, E. Skordeva, D. Arsova, M. Nikiforova (1987), Optical properties of Ge-As-S thin films, *J.Non-Cryst. Solids*, 90, pp.481-485.

S. Elliott (1984), Physics of Amorphous Materials, Longman Inc., New York, 155, pp.98.

R. Elliot and A.Gibson (1974), An Introduction to Solid State Physics and Application, 1st ed, Macillian Inc, 471, p.92.

J. Millman (1979) Microelectronics, Murray – Hill, Book Company Kogakusha, 642, pp.172.

B.Ray (1969) II-VI Compounds, Pergamon Press, 1st ed printed in Great Britain by Neil and Co. Ltd. of Edinburgh, pp.162.

S.Sze (1981) Physics of Semiconductor Devices, John Wiley and Sons, 109, pp.76.

K. Palanjyan, S. Messaddeq, Y. Messaddeq, R. Vallée, E. Knystautas, and T. Galstian (2013), Study of photoinduced birefringence vs As content in thin GeAsS films, *Optical Materials Express*, 3(6) pp. 671.

N. F. Mott, E. A. Davis (1982), Electron Processes in Non-Crystalline Materials, Mir, ,pp. 198.

R. Todorov (2003), Light- induced changes in the optical properties of thin films of Ge-S-Bi(Tl, In) chalcogenides., *Journal of Non-Crystalline Solids*, 326&327, pp.263-267.

K. Petkov (2002), Compitinal dependence of the photoinduced phenomena in thin chalcogenide films, *Journal of Optoelectronics and Advanced Materials*, 4(3) pp. 611 – 629.

Jia Zhu, Zongfu Yu, George F. Burkhard, Ching-Mei Hsu, et al (2009), Optical Absorption Enhancement in Amorphous Silicon Nanowire and Nanocone Arrays, *Nano Letters*, 9(1) PP.279-282.

Z. G. Ivanova, P. Petkova, V. S. Vassileva (2001), Optical and electrical properties of amorphous $GeS_2)_{100-x}$-Ga_x. thin films, *Journal of Optoelectronics and Advanced Materials*, 3(2), pp. 481 – 484.

C. T. Sah, R. N. Noyce and W. Shockley W(1957), *Proc. IRE,* 45, pp.1228–43.

O. Breitenstein, P. P. Altermatt, K. Ramspeck and A.Schenk (4-8 sep.2006), THE origin of ideality factors N > 2 OF Shunts and surfaces in the dark I-V curves of si solar cell, 21st European Photovoltaic Solar Energy Conference, 4-8 September 2006, Dresden, Germany *21st European Photovoltaic Solar Energy Conference*, Dresden, Germany. pp 625–28

A. Schenk, and U. Krumbein (1995), Coupled defect-level recombination: theory and applica- tion to anomalous diode characteristics, *J. Appl. Phys.,* 78, pp.3185-92.

M. Brotzmann , Vetter U and Hofs¨ass H (2009), BN/ZnO Heterojuntion diodes with apparently giant ideality factors, *J. Appl. Phys.*,106, 063704.

Xu Z, Yoon S F, Yeo Y C, Chia C K, Cheng Y Band Dalapati G K (2012), characterization of thin films GaAs diodes grown on germanium-on-insulator on Si substrate, *J. Appl. Phys.,* 111, pp. 044504-1-4.